



Impact of different tissue dissociation protocols on endothelial cell recovery from developing mouse lungs

Francesco Palumbo^{1,2,3} | Miša Gunjak^{2,3,4} | Patty J. Lee⁵ |
Stefan Günther⁶ | Anne Hilgendorff^{7,8} | István Vadász^{3,9,10} |
Susanne Herold^{9,10,11} | Werner Seeger^{2,3,9,10} | Christian Mühlfeld¹² |
Rory E. Morty⁴

¹Flow Cytometry Core Facility, School of Life Sciences, École Polytechnique Fédérale de Lausanne (EPFL), Lausanne, Switzerland

²Department of Lung Development and Remodelling, Max Planck Institute for Heart and Lung Research, Bad Nauheim, member of the German Center for Lung Research (DZL), Bad Nauheim, Germany

³Department of Internal Medicine (Pulmonology), University of Giessen and Marburg Lung Center (UGMLC), member of the German Center for Lung Research (DZL), Justus Liebig University Giessen, Giessen, Germany

⁴Department of Translational Pulmonology and the Translational Lung Research Center Heidelberg (TLRC), Heidelberg University Hospital, member of the German Center for Lung Research (DZL), Heidelberg, Germany

⁵Division of Pulmonary, Critical Care and Sleep Medicine, Icahn School of Medicine at Mount Sinai, New York, New York, USA

⁶Deep Sequencing Platform, Max Planck Institute for Heart and Lung Research, Bad Nauheim, member of the German Center for Lung Research (DZL), Bad Nauheim, Germany

⁷Institute for Lung Health and Immunity and Comprehensive Pneumology Center (CPC), Helmholtz Zentrum München, member of the German Center for Lung Research (DZL), Munich, Germany

⁸Center for Comprehensive Developmental Care (CDeCLMU) at the Social Pediatric Center, Dr. von Hauner Children's Hospital, Ludwig-Maximilian-University, Munich, Germany

⁹Institute for Lung Health, Justus Liebig University Giessen, Giessen, Germany

¹⁰Cardio-Pulmonary Institute, Justus Liebig University Giessen, Giessen, Germany

¹¹Department of Internal Medicine (Infectious Disease and Hospital Hygiene), University of Giessen and Marburg Lung Center (UGMLC), member of the German Center for Lung Research (DZL), Justus Liebig University Giessen, Giessen, Germany

¹²Institute of Functional and Applied Anatomy and Biomedical Research in Endstage and Obstructive Lung Disease Hannover (BREATH), Hannover Medical School, member of the German Center for Lung Research (DZL), Hannover, Germany

Correspondence

Rory E. Morty, Department of Translational Pulmonology, Heidelberg University Hospital, Im Neuenheimer Feld 156, 69120 Heidelberg, Germany.

Email: rory.morty@med.uni-heidelberg.de

Funding information

German Federal Ministry of Education and Research; German Research Foundation, Grant/Award Numbers: 197785619, 114933180, 284237345, 390649896, 420759458; Heidelberg University Hospital; Hessian Ministry of Higher Education, Research and the Arts, Grant/Award Number: III L7-519/05.00.002; Max Planck Society; Medical Faculty of the University of

Abstract

Flow cytometry and fluorescence-activated cell sorting are widely used to study endothelial cells, for which the generation of viable single-cell suspensions is an essential first step. Two enzymatic approaches, collagenase A and dispase, are widely employed for endothelial cell isolation. In this study, the utility of both enzymatic approaches, alone and in combination, for endothelial cell isolation from juvenile and adult mouse lungs was assessed, considering the number, viability, and subtype composition of recovered endothelial cell pools. Collagenase A yielded an 8-12-fold superior recovery of viable endothelial cells from lung tissue from developing mouse pups, compared to dispase, although dispase proved superior in efficiency for epithelial cell recovery. Single-cell RNA-Seq revealed that the collagenase A approach yielded a

This is an open access article under the terms of the [Creative Commons Attribution-NonCommercial](https://creativecommons.org/licenses/by-nc/4.0/) License, which permits use, distribution and reproduction in any medium, provided the original work is properly cited and is not used for commercial purposes.

© 2024 The Authors. *Cytometry Part A* published by Wiley Periodicals LLC on behalf of International Society for Advancement of Cytometry.

Heidelberg; U.S. National Heart, Lung and Blood Institute of the National Institutes of Health, Grant/Award Number: R01HL138386; U.S. Department of Veterans Affairs, Grant/Award Number: VAORD11858595; U.S. Department of Defense, Grant/Award Number: PR150809; von Berhing-Röntgen Foundation, Grant/Award Number: 66-LV07

diverse endothelial cell subtype composition of recovered endothelial cell pools, with broad representation of arterial, capillary, venous, and lymphatic lung endothelial cells; while the dispase approach yielded a recovered endothelial cell pool highly enriched for one subset of general capillary endothelial cells, but poor representation of other endothelial cells subtypes. These data indicate that tissue dissociation markedly influences the recovery of endothelial cells, and the endothelial subtype composition of recovered endothelial cell pools, as assessed by single-cell RNA-Seq.

KEYWORDS

endothelial cell, endothelial cell subset, flow cytometry, lung, lung development, mouse, protocol, single-cell analysis, single-cell RNA-seq, tissue dissociation

1 | INTRODUCTION

Lung endothelial cells are credited with a driving role in normal and aberrant pre [1] and postnatal [2–6] development of the lung architecture as well as in pulmonary hypertension in the preterm and term neonate and infants [7]. Lung endothelial cells also play a pivotal role in lung homeostasis [8] and the development and progression of a spectrum of adult lung diseases [9], including the sexual dimorphism noted in lung disease [10, 11]. Thus, exploitation of the lung endothelial niche is seen as a potential avenue for promoting the regeneration of diseased lungs [12]. For these reasons, there is tremendous scope for the application of flow cytometry and fluorescence-activated cell sorting (FACS) in studies on endothelial cell function in lung development, homeostasis, and disease. To this end, flow-cytometry based methods have been developed to efficiently separate major human lung cell populations [13], and the comprehensive phenotyping of both mouse [14] and human [15] endothelial cells by flow cytometry has been reported in the pages of this journal. Furthermore, a comprehensive organ-wide (“atlas”) phenotyping study of mouse endothelial cells has been undertaken [16] and an integrated single-cell atlas of human lung endothelial cells has been generated [17, 18]. A tranche of recent reports has also considerably expanded our appreciation of the subtypes of endothelial cells in adult mouse lungs [19], and the developing mouse lung [20], with a number of subtypes and “subtypes of subtypes” of lung endothelial cells having been described and characterized [21], although much functional work on these cells remains to be done.

The surge of interest in identifying, characterizing, and assigning functions to endothelial cell subtypes in the lung, in particular, in the developing lung, has led to a number of investigators generating endothelial cell isolation protocols in parallel. Notable among these are tissue dissociation protocols based on enzymatic digestion of lung tissue [22] to liberate endothelial (and other) cells to facilitate flow cytometric analyses and FACS isolation of endothelial cells for single-cell RNA-Seq studies. Most commonly, preparations of bacterial collagenases such as collagenase A from *Clostridium histolyticum* and a neutral metalloproteinase from *Bacillus polymyxa* are employed, either alone, or mixed together, with some investigators also including porcine elastase [16, 21, 23–27].

To date, it is not known whether different enzymatic digestion protocols might impact endothelial cell recovery, viability, or the subtype composition of recovered endothelial cell pools. This would be important to determine, since an impact of tissue dissociation on recovery and cell phenotype might impact the comparison of data between groups, and indeed, one method may be preferable to another. A recent American Thoracic Society Workshop Report on “Improving the Quality and Reproducibility of Flow Cytometry in the Lung” has highlighted concerns about the accuracy and reproducibility of flow cytometry studies as being significant hurdles to the scientific advances that can be achieved using this powerful technology [28]. Underscoring this concern, a recent report in this journal documented how different dissociation protocols quantitatively and qualitatively impact recovery of a spectrum of cell-types in single-cell suspensions from peripheral human lung tissue [29]. With that in mind, the objective of the present study was to compare the utility of the two most widely used enzymatic tissue dissociation reagents for the isolation of lung endothelial cells.

2 | MATERIALS AND METHODS

2.1 | Lung tissue processing using collagenase and dispase

Wild-type C57BL/6J mice were obtained from Janvier (Le Genest-Saint-Isle, France). Mice were maintained on a 12 h/12 h day/night cycle and provided with food and water ad libitum. Mice were maintained and killed as approved by the *Regierungspräsidium Darmstadt*, the competent legal authority that oversees experimental animal studies at the Max Planck Institute for Heart and Lung Research in Bad Nauheim, Germany. Mouse pups were killed on the 14th day or 22 week of postnatal life with an intraperitoneal injection of sodium pentobarbital (500 mg/kg; Narcoren®, Boehringer Ingelheim, Ingelheim am Rhein, Germany). The lungs and heart were exposed by mid-sternal thoracotomy, and lungs were perfused with phosphate-buffered saline (PBS) via the left ventricle using a hand-held 20 mL syringe. Lungs were excised *en bloc*, briefly immersed in serum-free Roswell Park Memorial Institute (RPMI) cell-culture medium (Thermo

Fisher, Waltham, MA, USA), placed in a Petri dish, and manually minced using fine surgical scissors. Lung fragments were transferred into a 50 mL Falcon tube containing digestion solution. For collagenase digestion, a 0.01% (m/v) solution of *Clostridium histolyticum* collagenase A (officially, “microbial collagenase”, EC 3.4.24.3; 10103586001; Merck, Darmstadt, Germany) was prepared in serum-free RPMI (total volume, 30 mL) and incubated for 10 min. For dispase digestion, a commercially-available preparation of dispase, which contains a purified preparation of *Bacillus polymyxa* neutral metalloproteinase (officially, “bacillolysin”, EC 3.4.24.28; CLS354235; Merck, Darmstadt, Germany) was employed at a concentration of 125 U in 30 mL serum-free RPMI. Lung tissue was then incubated at 37°C with gentle agitation on a Bio RS-24 Mini-rotator (Biosan, Riga, Latvia) for 10 min. In one group of studies, the collagenase A and the dispase were combined together, each at the same concentrations as were employed in the single-enzyme studies. Additionally, the three enzymatic digestions protocols were undertaken using adult (22 week old, female) mouse lungs, in which case the incubation time was increased to 15 min. Lung tissue was homogenized by passage 10× through a 20 mL syringe fitted with an 18 G needle. The cell suspension was filtered through a 150 µm, followed by a 70 µm, and followed by a 40 µm filter (all from Carl Roth, Karlsruhe, Germany) into a 50 mL Falcon tube, which was centrifuged at 1000 × g for 5 min at 4°C. The cell pellet was washed 1× in Ham's F12 medium (Thermo Fisher, Waltham, MA, USA) containing 10% (v/v) fetal bovine serum and 320 U/mL DNase I (Serva, Heidelberg, Germany) [22], recentrifuged, and resuspended in eBioscience™ Flow Cytometry Staining Buffer (00-4222-26; Thermo Fisher, Waltham, MA, USA).

2.2 | Cell staining and processing

Cell suspensions were first incubated with BD Pharmingen™ Purified Rat Anti-Mouse CD16/CD32 (Mouse BD Fc Block™, 553142; BD BioSciences, Heidelberg, Germany) for 5 min at room temperature. For CD31 staining, cell suspensions were incubated together with PE-coupled anti-mouse CD31 (102508, BioLegend, San Diego, CA, USA; 1:200) and APC-coupled anti-mouse CD45 Antibody (147708, BioLegend, San Diego, CA, USA; 1:200) for 20 min at 4°C. Cell suspensions were centrifuged at 1000 × g for 5 min at 4°C. The cell pellet was washed 1× in eBioscience™ Flow Cytometry Staining Buffer and resuspended in 3 mL Ham's F12 medium containing 10% (v/v) fetal bovine serum and 320 U/mL bovine pancreas DNase I (18535.02; Serva, Heidelberg, Germany). For EpCam staining, cell suspensions were incubated with FITC-coupled anti-mouse CD326 (EpCAM) antibody (118207, BioLegend, San Diego, CA, USA; 1:200) for 20 min at 4°C. In selected instances, samples were stained with DAPI (0.2 µg/mL) prior to analysis. For Hoechst 3342 staining, the Hoechst staining was undertaken prior to antibody staining: cell suspensions were incubated in 2 µg/mL Hoechst 3342 (H3570; Thermo Fisher, Waltham, MA, USA) for 40 min at 37°C, and staining for CD31 and CD45 was then undertaken as described above, without any subsequent DAPI staining. Annexin V staining was undertaken after CD31 and CD45

staining, by washing the anti-CD31/CD45 stained cells 1× with Annexin V Binding Buffer (422201; BioLegend, San Diego, CA, USA), resuspended in the same buffer (400 µL) and incubated with FITC-coupled Annexin V (640906, BioLegend, San Diego, CA, USA; 1:20) for 15 min at room temperature, in the dark.

2.3 | Flow cytometry

Stained cell suspensions were analyzed on a BD LSRFortessa™ or a BD FACSymphony A1 Cell Analyzer (BD BioSciences, Heidelberg, Germany). Samples were acquired at a low speed, with approximately 1200 events/s. For each experiment, 500,000 events per condition were acquired, with the exception of the data presented in Figure 1, where 100,000 events were acquired per condition, and the data in Figure 7, where 300,000 events were acquired per condition. Forward scatter was detected using a blue laser (λ, 488 nm) with a neutral density filter (2.0 mm) placed in front of the 488/20 bandpass filter. Side scatter was detected using a blue laser (λ, 488 nm) using a 488/10 bandpass filter. The FITC signal was detected with a blue laser (λ, 488 nm) using a 530/30 bandpass filter. The APC signal was detected with a red laser (λ, 640 nm) using a 670/30 bandpass filter. The PE signal was detected with a yellow/green laser (λ, 561 nm) using a 586/15 bandpass filter. Both DAPI and Hoechst 33342 signals were detected using a UV laser (λ, 355 nm) using a 450/50 bandpass filter. Voltages were adjusted based on the signals obtained for unstained samples.

Gating strategies were determined using unstained and single-stained controls, as described for CD31, CD45, DAPI, and annexin V staining of lung endothelial cells (Figure S1), for Hoechst 3342 staining of lung endothelial cells (Figure S2), and for EpCam and DAPI staining of lung epithelial cells (Figure S3).

2.4 | Single-cell RNA-Seq

Endothelial cell fractions were prepared from single-cell suspensions for single-cell RNA-Seq analysis by FACS. Cell staining was undertaken exactly as described for the CD31/CD45/DAPI staining in Section 2.2. Cells were sorted on a BD FACSAria II (BD Biosciences, Heidelberg, Germany), using the same configurations as those described for the BD LSRFortessa in Section 2.3. From the single-cell suspensions, 100,000 endothelial cells were obtained for each of the two tissue digest conditions.

The single-cell suspensions were processed using Chromium Next GEM Single-Cell 3' Reagent Kit v3.1 (10× Genomics, San Francisco, California, USA). Single-cell partitioning and barcoding was undertaken using a 10× genomics chromium controller, and gene expression libraries were prepared according to the manufacturer's instructions.

Sequencing was performed using a Nextseq2000 sequencing system (Illumina, San Diego, California, USA), and raw reads were aligned against the *Mus musculus* genome (Genome Reference Consortium Mouse Build 38; available under GenBank accession number GCA_000001635.2) and counted using StarSolo [30, 31] (available at

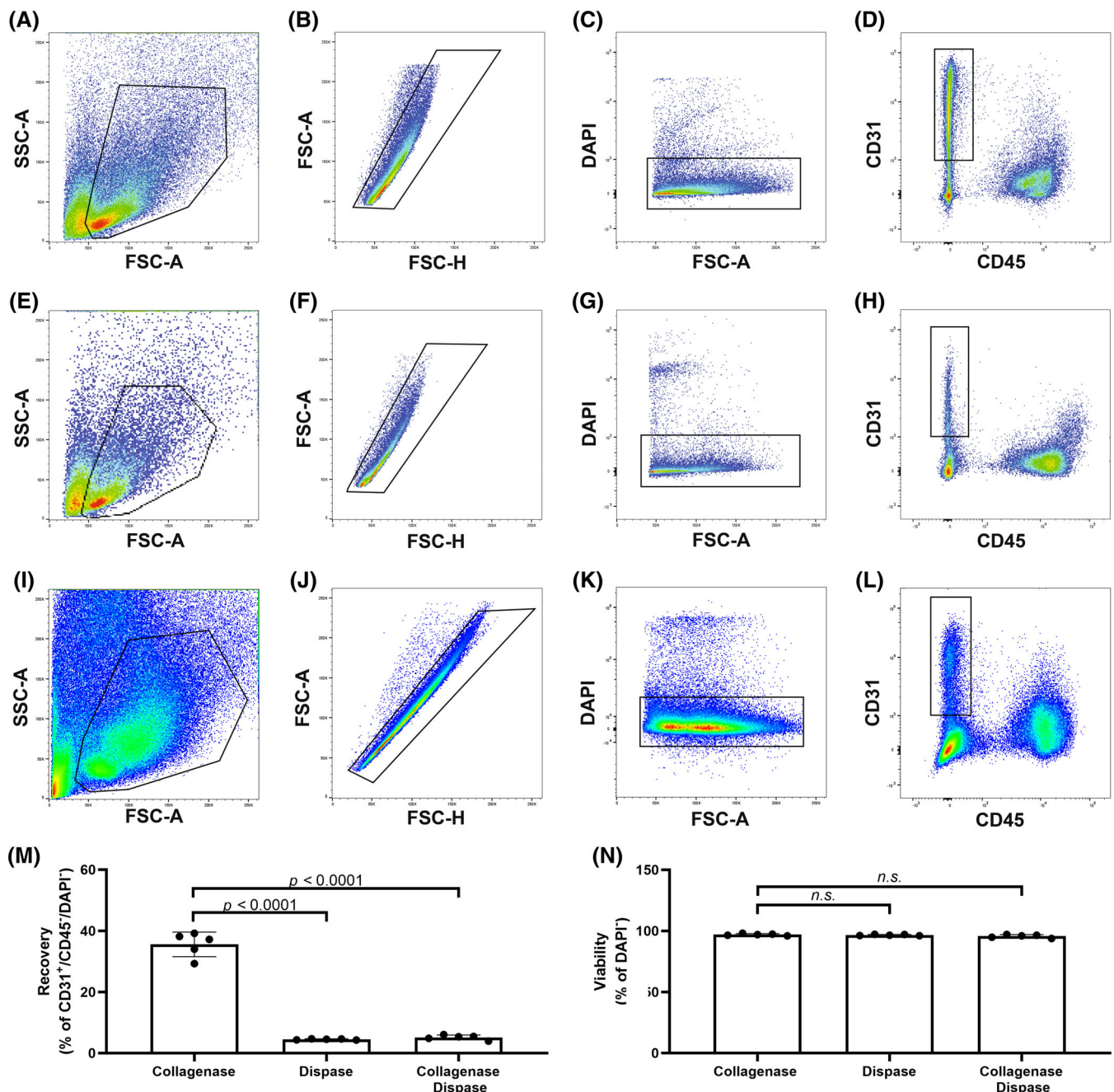


FIGURE 1 Recovery of live lung endothelial cells comparing collagenase-based and dispase-based tissue dissociation protocols using DAPI exclusion. Live endothelial cells were identified by flow cytometry in single-cell suspensions prepared from lung tissue of 14-day old mice that was dissociated using either collagenase (A–D) or dispase (E–H), or combinations thereof (I–L). Primary debris exclusion was undertaken by SSC-A versus FCS-A gating (A, E, I), followed by doublet exclusion using FSC-A versus FSC-H gating (B, F, J). Live cells were identified by DAPI exclusion, thus, represented by DAPI⁻ events (C, G, K), and CD31⁺/CD45⁻ events represented endothelial cells (D, H, L). Live endothelial cell recovery was assessed as (M) a percentage of CD31⁺/CD45⁻/DAPI⁻ events: the gated populations in C versus D, G versus H, or K versus L. The viability of the whole single-cell suspension was assessed as (N) a percentage of DAPI⁻ events in the singlet cell population event gate: the gated populations in C versus B, G versus F, and K versus J. For each cell population, 100,000 events were assessed ($n = 5$ experimental animals per group). Statistical comparisons were made using a one-way ANOVA with Tukey's post hoc test. $p < 0.05$ was considered significant. n.s., not significant [Correction added after first online publication on 15 May 2024. Figure 1 has been updated with labeling on the X axis of parts A–D and F–H.]. [Color figure can be viewed at [wileyonlinelibrary.com](https://onlinelibrary.wiley.com)]

www.github.com). Preprocessed counts were further analyzed using single-cell analysis in Python (Scanpy) [32] (available at www.github.com), followed by a secondary analysis in Annotated Data Format. Cell

quality control was conducted by taking the number of detected genes and mitochondrial content into consideration. A total of 168 cells were removed, which did not express more than 300 genes or which exhibited

a mitochondrial content greater than 3.5%. Additionally, 13,018 genes were filtered out as those genes were detected in less than 30 cells. The total number of cells presented in the single-cell analyses were 8304 cells (collagenase group), and 4814 cells (dispase group). Raw counts per cell were normalized to the median count across all cells and transformed into log space to stabilize variance. The dimensionality of the dataset was initially reduced using PCA, retaining 50 principal components. Subsequent analyses, including low-dimensional uniform manifold approximation and projection (UMAP) embedding (<https://arxiv.org/abs/1802.03426>) and cell clustering via community detection were based on the initial principal component analysis (PCA). Final data visualization was done using both the scanpy and CELLxGENE (available from <https://cellxgene.cziscience.com/>) packages.

Single-cell RNA datasets were deposited in the GEO database under accession number GSE236874 (<https://www.ncbi.nlm.nih.gov/geo/query/acc.cgi?acc=GSE236874>).

2.5 | Data analysis

All flow cytometry and FACS data were analyzed with FlowJo version 10.8.1. (FlowJo, Ashland, OR, USA). Statistical analysis of flow cytometry data was undertaken with Prism (GraphPad Software, Boston, MA, USA), using either an unpaired Student's *t* test or a one-way ANOVA with Tukey's post hoc test. A $p < 0.05$ was considered significant.

3 | RESULTS

3.1 | Impact of enzymatic tissue dissociation on live endothelial cell recovery from the lungs of developing mouse pups

Lungs that were harvested from mouse pups on the 14th day of post-natal life were dissociated using either collagenase or dispase or a combination of the two, and cell debris was excluded using SSC-A versus FSC-A gates (Figure 1A,E,I). Singlet cells were separated from higher-order aggregates using FSC-A versus FSC-H gates (Figure 1B,F,J). Live cells were initially identified by DAPI exclusion using DAPI versus FSC-A gates (Figure 1C,G,K), and within that population, CD31⁺ endothelial cells were delineated from CD45⁺ inflammatory cells (Figure 1D,H,L). The recovery of live endothelial cells was higher in collagenase-generated cell preparations than in dispase-generated cell populations (35.58 ± 4.02% vs. 4.50 ± 0.18%, $p < 0.0001$; Figure 1M). However, within the parent cell population as a whole (gated events in Figure 1C,G,K; which contains endothelial, epithelial, inflammatory, and other cells) there was no difference in the proportion of live cells as a fraction of the parent cell populations (gated events in Figure 1B,F,J, respectively, representing the single-cell suspension) as illustrated in Figure 1N. A combination of collagenase and dispase yielded comparable endothelial cell recovery to when dispase was employed alone (Figure 1M and Figure 1N).

In a parallel set of analyses, instead of DAPI exclusion, Hoechst 3342 inclusion was employed to identify live cells. As with the DAPI

studies, mouse lung tissue was dissociated using either collagenase or dispase, cell debris was excluded using SSC-A versus FSC-A gates (Figure 2A,E), and singlet cells were separated from higher-order aggregates using FSC-A versus FSC-H gates (Figure 2B,F). Departing from the DAPI protocol, live cells were identified by Hoechst 3342 inclusion using Hoechst-A versus Hoechst-W gates (Figure 2C,G), and within that Hoechst 3342⁺ population, CD31⁺ endothelial cells were delineated from CD45⁺ inflammatory cells (Figure 2D,H). As with the DAPI studies, the recovery of live endothelial cells was higher in collagenase-generated cell preparations than in dispase-generated cell populations (86.06 ± 3.32% vs. 76.60 ± 4.41%, $p = 0.0029$; Figure 2I). However, in contrast to the DAPI studies, within the parent cell population as a whole (gated events in Figure 2C,G; which contains endothelial, epithelial, inflammatory, and other cells) the recovery of live cells was higher in collagenase-generated cell preparations than in dispase-generated cell populations (19.280 ± 2.681% vs. 1.664 ± 0.314%, $p < 0.0001$; Figure 2J) when viewed as a proportion of the parent cell populations, the starting single-cell suspensions (gated events in Figure 2B,F, respectively).

3.2 | Impact of collagenase- versus dispase-based tissue dissociation on endothelial cell apoptosis

Following mouse pup lung tissue dissociation using either collagenase or dispase, cell debris was excluded using SSC-A versus FSC-A gates (Figure 3A,E), singlet cells were separated from higher-order aggregates using FSC-A versus FSC-H gates (Figure 3B,F), and within that population, CD31⁺ endothelial cells were delineated from CD45⁺ inflammatory cells (Figure 3C,H). The onset of early apoptosis, detected by annexin V positivity, was then assessed alongside live/dead cell discrimination using DAPI (Figure 3D,J), and the CD31⁺/CD45⁻ population within the DAPI⁻/annexin V gated population was reassessed using back-gating (Figure 3E,K). The proportion of apoptotic live endothelial cells [assessed as the proportion of annexin V⁺/DAPI⁻ events (gated population in Figure 3D,J) in the gated CD31⁺/CD45⁻ population in Figure 3C,H, respectively] was greater (26.85 ± 4.42% vs. 12.21 ± 3.17%; $p = 0.0003$) in the collagenase-generated cell suspensions than in the dispase-generated cell suspensions (Figure 3L). Similarly, the total number of apoptotic, live endothelial cells (assessed as annexin V⁺/DAPI⁻ events within 500,000 events) in the collagenase-generated cell populations was greater (15,926 ± 3434 vs. 953 ± 237; $p < 0.0001$) in the collagenase-generated cell suspensions than in the dispase-generated cell suspensions (Figure 3M).

3.3 | Impact of enzymatic tissue dissociation on live epithelial cell recovery

Lungs that were harvested from mouse pups on the 14th day of post-natal life were dissociated using either collagenase, dispase, or combinations thereof, and cell debris was excluded using SSC-A versus FSC-A gates (Figure 4A-C). Singlet cells were separated from higher-order aggregates using FSC-A versus FSC-H gates (Figure 4D-F). Live epithelial cells were identified by DAPI exclusion using DAPI versus

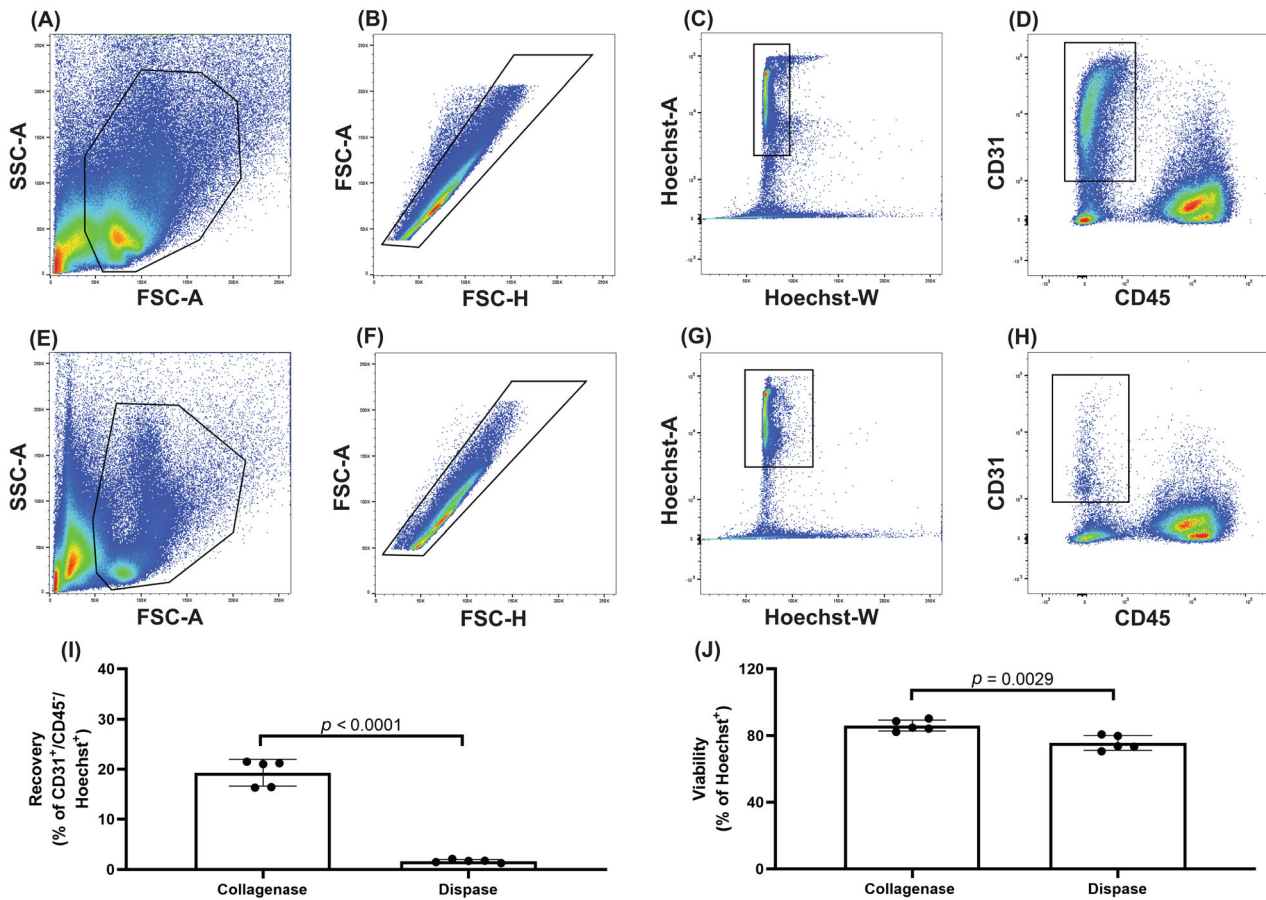


FIGURE 2 Recovery of live lung endothelial cells comparing collagenase-based and dispase-based tissue dissociation protocols using Hoechst 33342 positive selection. Live endothelial cells were identified by flow cytometry in single-cell suspensions prepared from lung tissue of 14-day old mice that was dissociated using either collagenase (A–D) or dispase (E–H). Primary debris exclusion was undertaken by SSC-A versus FCS-A gating (A, E), followed by doublet exclusion using FSC-A versus FSC-H gating (B, F). Live cells were identified by Hoechst 33342 (Hoechst) inclusion, thus, represented by Hoechst⁺ events (C, G), and CD31⁺/CD45⁻ events represented endothelial cells (D, H). Live endothelial cell recovery was assessed as (I) a percentage of CD31⁺/CD45⁻/Hoechst⁺ events: the gated populations in C versus D, or G versus H. The viability of the entire singlet cell single-cell suspension was assessed as (J) a percentage of Hoechst⁺ events in the singlet cell population event gate: the gated populations in C versus B, and G versus F. For each cell population, 500,000 events were assessed ($n = 5$ experimental animals per group). Statistical comparisons were made using an unpaired Student's *t* test. $p < 0.05$ was considered significant. [Color figure can be viewed at [wileyonlinelibrary.com](https://onlinelibrary.wiley.com/doi/10.1002/cyto.a.24883)]

EpCam gates (Figure 4G–I). The recovery of live epithelial cells was higher in dispase-generated cell preparations than in collagenase-generated cell populations ($1.842 \pm 0.239\%$ vs. $15.80 \pm 1.05\%$, $p < 0.0001$; Figure 4J), when viewed as a proportion of the EpCam⁺/DAPI⁻ parent cell population (gated events in Figure 4G,H, respectively) or as a comparison of the total number of EpCam⁺/DAPI⁻ events within 500,000 events (2479 ± 694 vs. $14,765 \pm 4363$ events, $p < 0.0001$; Figure 4K). A combination of collagenase and dispase did not exhibit an appreciable impact on epithelial cell recovery, when compared to the collagenase alone or dispase alone protocols (Figure 4J,K).

3.4 | Impact of collagenase- versus dispase-based tissue dissociation on the endothelial subpopulation composition of endothelial cell pools

Endothelial cell populations isolated using either the collagenase-based or dispase-based approaches were sorted by FACS

and subjected to single-cell RNA-Seq to identify endothelial cell subpopulations. The single-cell RNA-Seq datasets have been deposited in the GEO Database under accession number GSE236874. Using PCA, a UMAP identified analysis nine endothelial cell subpopulations in the endothelial cell preparations (Figure 5A), and differential abundance of the subpopulations within the endothelial cell pool as a whole comparing the collagenase- (Figure 5B) and dispase-based (Figure 5C) approaches. The endothelial cell pools included three subpopulations of arterial endothelial cells, three populations of capillary endothelial cell populations, lymphatic vessel endothelial cells, endothelial progenitor cells, and venous endothelial cells (Figure 5D). The collagenase-based approach yielded a diverse endothelial subpopulation pool (Figure 5E), while the dispase-based approach yielded an endothelial pool specifically enriched in one subpopulation of capillary endothelial cells termed gCap2 (Figure 5F). The differential gene expression within the endothelial cell subpopulations comparing endothelial cell pools generated using the collagenase- and dispase-based approaches is presented for selected genes that typify the nine

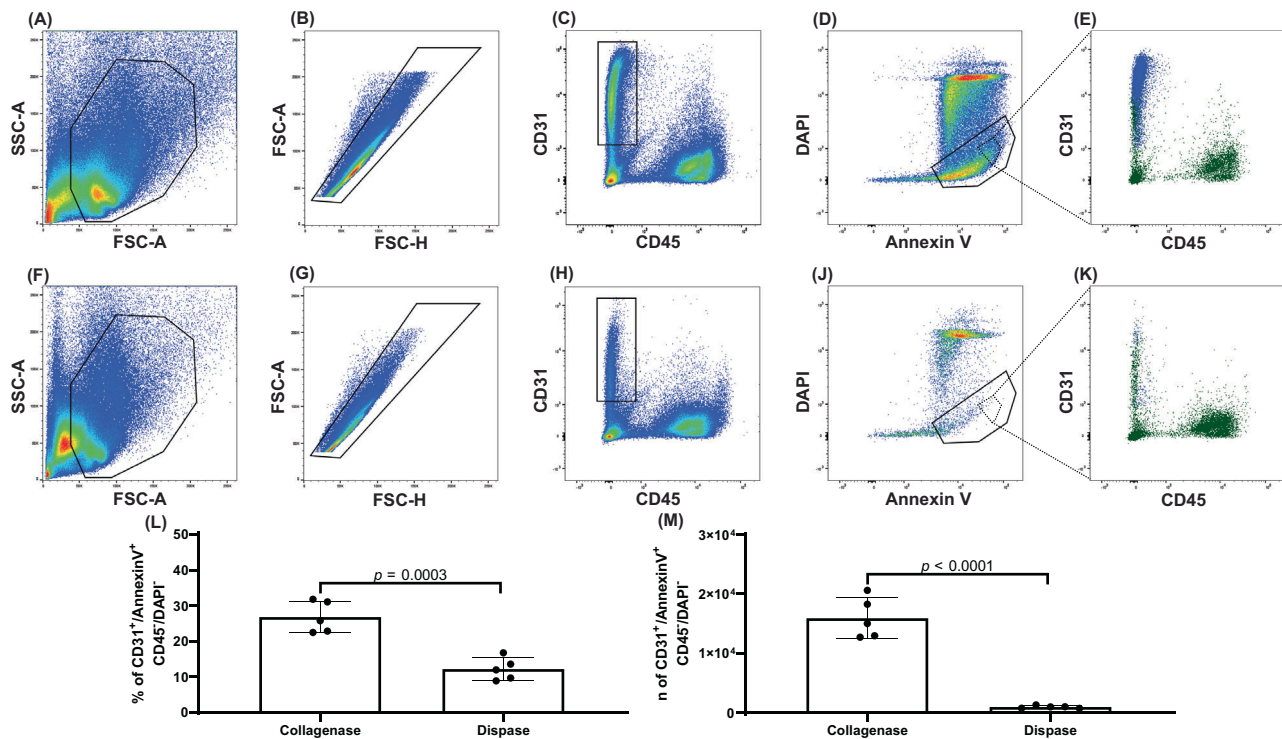


FIGURE 3 Apoptosis of live lung endothelial cells comparing collagenase-based and dispase-based tissue dissociation protocols using annexin V positive selection. Apoptosis in live endothelial cells was identified by flow cytometry in single-cell suspensions prepared from lung tissue of 14-day old mice that was dissociated using either collagenase (A–E) or dispase (F–K). Primary debris exclusion was undertaken by SSC-A versus FCS-A gating (A, F), followed by doublet exclusion using FSC-A versus FSC-H gating (B, G). Endothelial cells were represented by CD31⁺/CD45⁻ events (C, H), and live cells undergoing early apoptosis were identified by DAPI exclusion and annexin V positivity, thus, represented by DAPI⁻/annexin V⁺ events (D, J). The CD31⁺/CD45⁻ gated population was back-gated onto the DAPI⁻/annexin V⁺ population (E, K). Live endothelial cells undergoing early apoptosis were assessed as (L) a percentage of CD31⁺/annexin V⁺/CD45⁻/DAPI⁻ events: the gated populations in D versus C, or J versus H. (M) The absolute numbers of CD31⁺/annexin V⁺/CD45⁻/DAPI⁻ events in 500,000 events are also provided, from the gated populations in D and J. For each cell population, 500,000 events were assessed ($n = 5$ experimental animals per group). Statistical comparisons were made using an unpaired Student's *t* test. $p < 0.05$ was considered significant. [Color figure can be viewed at [wileyonlinelibrary.com](https://onlinelibrary.com)]

endothelial cell populations reported in Figure 5D–F are presented in Figure 5G–X. The characterization of the endothelial cell subtypes that constitute the endothelial cell pools generated using the collagenase- and dispase-based approaches is extended in Figure 6A–H, where violin plots reveal the differential expression of genes that are characteristic for endothelial cell subsets. Further to that, the expression patterns of representative genes that are diagnostic for the nine endothelial cell subtypes are presented in Figure 6I (dotplots) and Figure 6K (heatmaps). Additional gene expression data for classical endothelial markers genes are presented in Figure S4. These data reveal that the two different tissue dissociation protocols, one based on collagenase, and the other on dispase, generate endothelial cells pools of appreciably different subtype composition.

3.5 | Impact of enzymatic-based tissue dissociation on live endothelial cell recovery from adult mouse lungs

Lungs that were harvested from adult mice were dissociated using either collagenase or dispase or a combination of the two, and cell debris was excluded using SSC-A versus FSC-A gates (Figure 7A,E,I).

Singlet cells were separated from higher-order aggregates using FSC-A versus FSC-H gates (Figure 7B,F,J). Live cells were initially identified by DAPI exclusion using DAPI versus FSC-A gates (Figure 7C,G,K), and within that population, CD31⁺ endothelial cells were delineated from CD45⁺ inflammatory cells (Figure 7D,H,L). The recovery of live endothelial cells was higher in dispase-generated cell preparations than in collagenase-generated cell populations ($8.5158 \pm 1.15\%$ vs. $5.53 \pm 2.12\%$, $p = 0.0158$; Figure 7M). However, within the parent cell population as a whole (gated events in Figure 7C,G,K; which contains endothelial, epithelial, inflammatory, and other cells) there was no difference in the proportion of live cells as a fraction of the parent cell populations (gated events in Figure 7B,F,J, respectively, representing the single-cell suspension) as illustrated in Figure 7N. A combination of collagenase and dispase yielded comparable endothelial cell recovery to when either collagenase or dispase were employed alone (Figure 7M and Figure 7N).

4 | DISCUSSION

Lung endothelial cells are pivotal players in lung development, homeostasis, and disease. Thus, there is strong interest in the

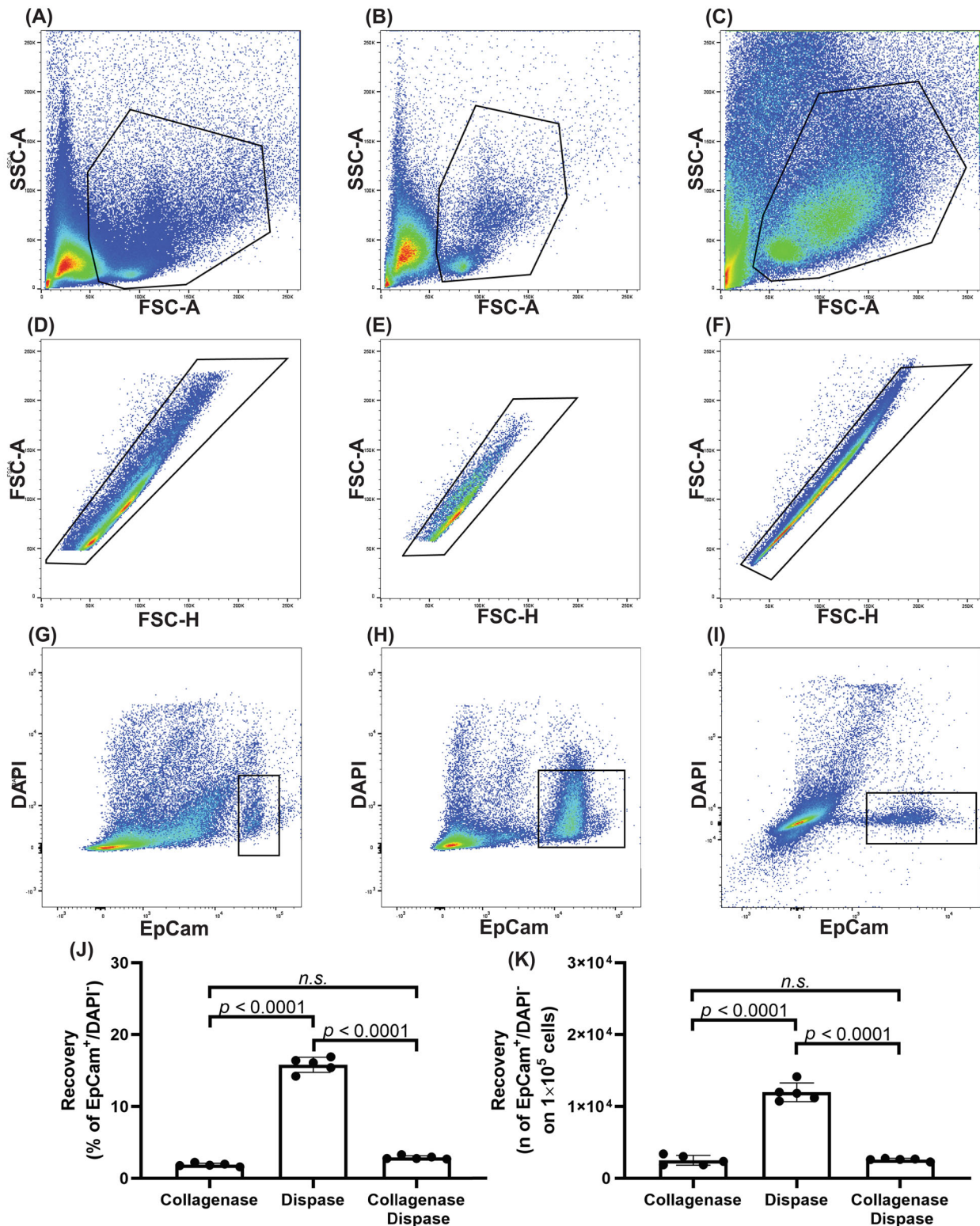


FIGURE 4 Recovery of live lung epithelial cells comparing collagenase-based and dispase-based tissue dissociation protocols using DAPI exclusion. Live epithelial cells were identified by flow cytometry in single-cell suspensions prepared from lung tissue of 14-day old mice that was dissociated using either collagenase (A, D, G), dispase (B, E, H), or a mixture thereof (C, F, I). Primary debris exclusion was undertaken by SSC-A versus FCS-A gating (A–C), followed by doublet exclusion using FSC-A versus FSC-H gating (D–F). Live cells were identified by DAPI exclusion, thus, represented by DAPI⁻ events (G–I) within the EpCam⁺ population. The recovery of live epithelial cells within the entire singlet cell single cell-suspension was assessed as (J) a percentage of EpCam⁺/DAPI⁻ events in the singlet cell population event gate: the gated populations in G versus D, H versus E, and I versus F. (K) The absolute numbers of EpCam⁺/DAPI⁻ events in 500,000 events are also provided, from the gated populations in G, H, and I. For each cell population, 500,000 events were assessed ($n = 5$ experimental animals per group). Statistical comparisons were made using a one-way ANOVA with Tukey's post hoc test. $p < 0.05$ was considered significant. [Color figure can be viewed at wileyonlinelibrary.com]

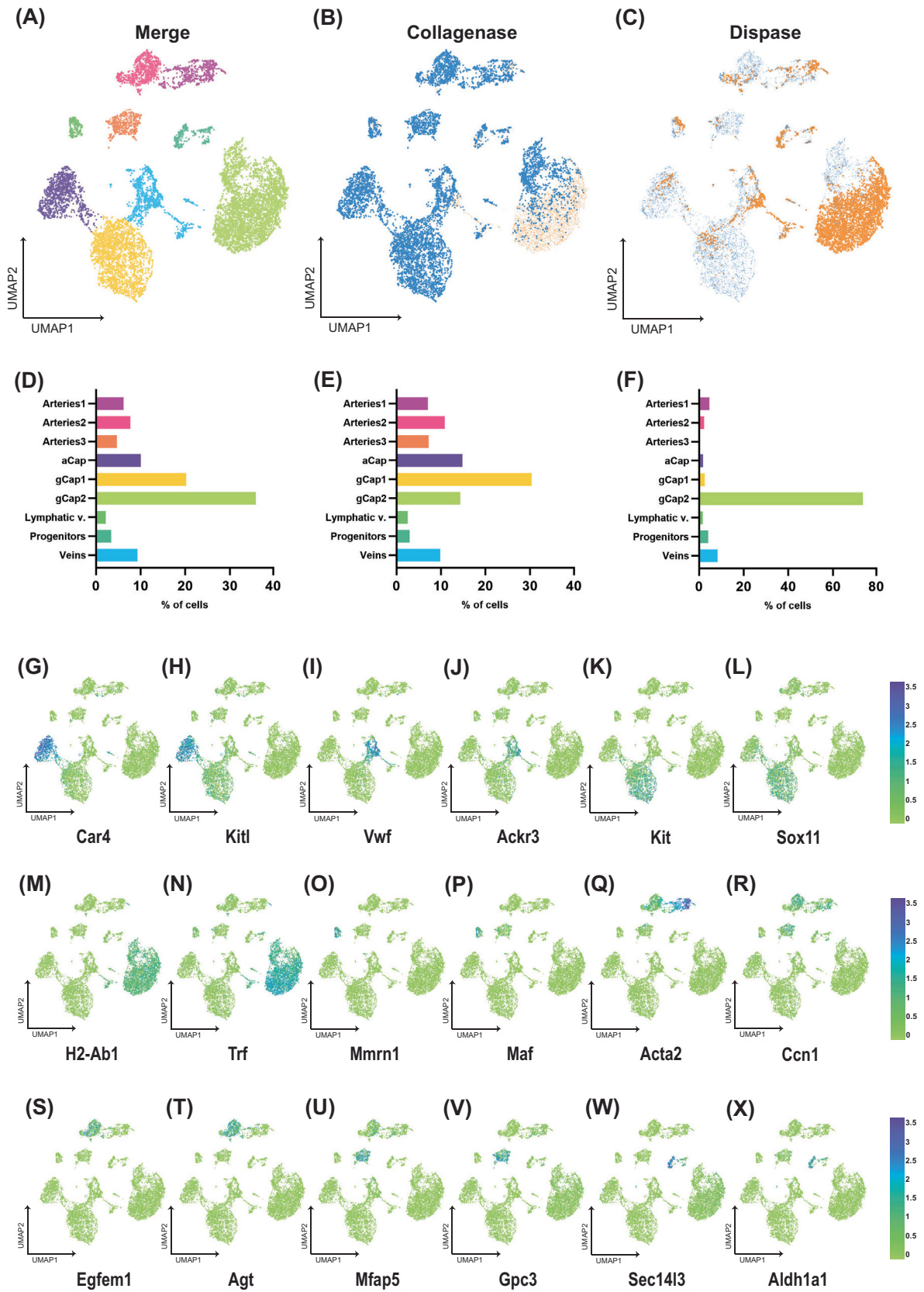


FIGURE 5 Legend on next page.

characterization of lung endothelial cells, and the preparative isolation of lung endothelial cells from animal models of lung development and disease, as well as from tissues obtained from affected patients. Because of the discriminatory power of flow cytometry and FACS, both methodologies are widely-employed in studies on lung developmental biology, for the quantification of lung endothelial cells, and the preparative isolation of lung endothelial cells for subsequent in vitro culture [33], DNA, RNA, or epigenetic analyses [11], and very likely in the future, for proteomic studies [34]. Given the surge of interest in the lung endothelial cell field, a number of approaches to endothelial cell isolation have been developed in parallel, by different investigators. A key step in the generation of single-cell suspensions from solid tissues is tissue dissociation, which is widely achieved for studies on lung cells using a variety of proteolytic enzymes, namely bacterial collagenases. To date, the lung endothelial community has employed either *C. histolyticum* collagenases [16], a commercial preparation of *B. polymyxa* neutral metalloproteinase, marketed as dispase [23], or mixtures thereof [24, 25]. These represent the most widely-used enzymatic lung dissociation protocols, although alternative approaches do exist, including other neutral metalloproteinases such as *Bacillus thermoproteolyticus* thermolysin, marketed as Liberase [26], a mixture of collagenase and porcine pancreatic elastase [27], as well as a mixture of collagenase, dispase, and elastase [21]. To address whether tissue dissociation protocols might influence the recovery of endothelial cells, or the constituent subpopulations of the recovered endothelial cell pool, the aim of the present study was to compare endothelial cell recovery, viability, apoptotic status, and heterogeneity of the recovered endothelial cell pools, using the two most commonly-employed tissue dissociation protocols for endothelial cell isolation: those based on collagenase and dispase.

For lungs harvested from young developing mouse pups, a comparison of endothelial cell recovery with collagenase versus dispase tissue dissociation protocols, using DAPI exclusion to identify live cells, revealed that the collagenase-based approach yielded eight-fold more live endothelial cells than did the dispase approach. The total number of live cells in the complete single-cell suspension (which includes inflammatory and epithelial cells) was comparable in both tissue dissociation protocols. A combination of collagenase and dispase negatively affected endothelial recovery compared to collagenase alone, indicating that the presence of dispase was deleterious for endothelial cell recovery. Several speculative ideas might be offered

to explain this. One possibility is that the immature extracellular matrix in mouse pup lungs is more susceptible to collagenase-mediated rather than dispase-mediated degradation, thus collagenase could liberate endothelial cells more effectively. However, that dispase (in the absence or presence of collagenase) had a negative impact implies that the dispase was destructive to the process, either by directly damaging endothelial cells, or altering the epitopes on endothelial cells from developing mouse lungs that were later used for endothelial cell detection by flow cytometry. Another possibility is that dispase alone could not liberate endothelial cells, and the dispase degraded the collagenase in a dispase-collagenase mixture, thus impeding endothelial cell liberation from tissue by collagenase.

Interestingly, when endothelial cells were liberated from adult mouse lung tissues, dispase, not collagenase, appeared to be the enzyme preparation of choice. This finding may reflect the maturation of the lungs themselves, or the maturation of the lung extracellular matrix. For example, the age of the young mouse pups (the 14th day of postnatal life) reflects an age that precedes the onset of the microvascular maturation stage of lung development, where the double capillary layer condenses into a single capillary layer [35]. Thus, the structural transformation of the lung between mouse pups and mouse adults is accompanied by marked changes in capillary endothelial cell arrangement and organization within the distal lung parenchyma. Furthermore, the maturation of the extracellular matrix proceeds over months and years. Elastin has a half-life of 70 years [36] and the kinetics of formation of different collagen cross-links are different, where the dehydrodihydroxylysinonorleucine cross-links form over days, while the hydroxylysyl pyridinoline cross-links form over weeks [37]. Thus, both the organization of lung endothelial cells, and the nature of the matrix in which lung endothelial cells is embedded are different, comparing juvenile mouse pups, and adult mice. This might impact the “extractability” of the cells using different enzymatic preparations for tissue digestion.

Conducting the same comparison, but using Hoechst 3342 inclusion, rather than DAPI exclusion, to identify live cells, revealed the same trend: collagenase tissue dissociation of lungs from developing mouse pups yielded 12-fold more (live) endothelial cells than did dispase tissue dissociation. These data further support our contention that the collagenase-based tissue dissociation protocol resulted in a substantial (8–12 fold) improvement in the recovery of (live) endothelial cells from mouse lungs in comparison to the dispase-based

FIGURE 5 Identification of live endothelial cell subpopulations comparing collagenase-based and dispase-based tissue dissociation protocols by single-cell RNA-Seq analysis. Live endothelial cell populations were obtained by fluorescence-activated cell sorting, as a CD31⁺/CD45⁻/DAPI⁻ population, gated according to negative controls (available in Figure S1). Cell populations were subjected to single-cell RNA-Seq analysis. A uniform manifold approximation and projection is provided for (A) the merged cell populations, where distinct endothelial cell subpopulations are indicated by colored cell clouds. (B) Endothelial cell subpopulations that are enriched in the collagenase- versus dispase-generated cell suspensions are colored in blue, while (C) the endothelial cell subpopulations enriched in the dispase-versus collagenase-generated cell suspensions are colored in orange, which an average of 6500 cells analyzed per group. The relative abundance of constituent cell populations in the projections presented in (A), (B), and (C) are presented in the corresponding panels (D), (E), and (F), respectively, where the bar color corresponds to the colors employed in (A). A comparison of the relative abundance of selected endothelial cell subtype marker genes in the projections is provided for (G) *Car4*, (H) *Kitl*, (I) *Vwf*, (J) *Ackr3*, (K) *Kit*, (L) *Sox11*, (M) *H2-Ab1*, (N) *Trf*, (O) *Mmrr1*, (P) *Maf*, (Q) *Acta2*, (R) *Ccn1*, (S) *Egfm1*, (T) *Agt*, (U) *Mfap5*, (V) *Gpc3*, (W) *Sec14l3*, (X) *Alhd1a1*. aCap, alveolar capillary; gCap, general capillary; v, vessels. [Color figure can be viewed at wileyonlinelibrary.com]

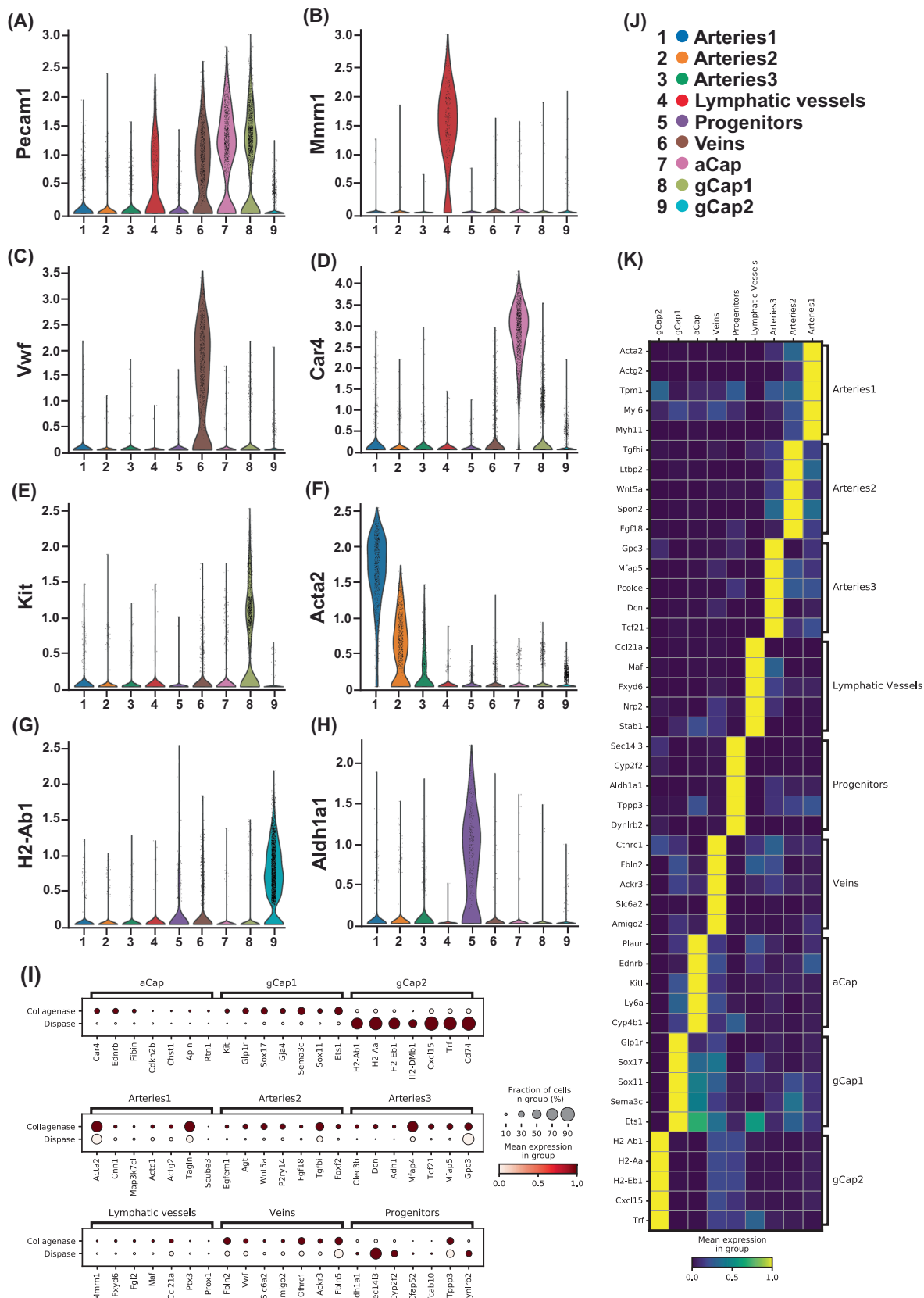


FIGURE 6 Differential expression of selected marker genes of endothelial subtype populations comparing collagenase versus dispase tissue dissociation protocols. The differential gene expression of genes commonly used to characterize the nine endothelial subpopulations described in Figure 5A are presented in violin plots for (A) *Pecam1*, (B) *Mmrn1*, (C) *Vwf*, (D) *Car4*, (E) *Kit*, (F) *Acta2*, (G) *H2-Ab1*, and (H) *Aldh1a1*. (I) The relative abundance of five genes that are collectively characteristic for each endothelial cell subpopulation are indicated in dotplots. (J) Color-code key for the data presented in (A–H), corresponding to the endothelial cell subpopulations identified in Figure 5A. (K) Heatmap of the data presented in (I). [Color figure can be viewed at wileyonlinelibrary.com]

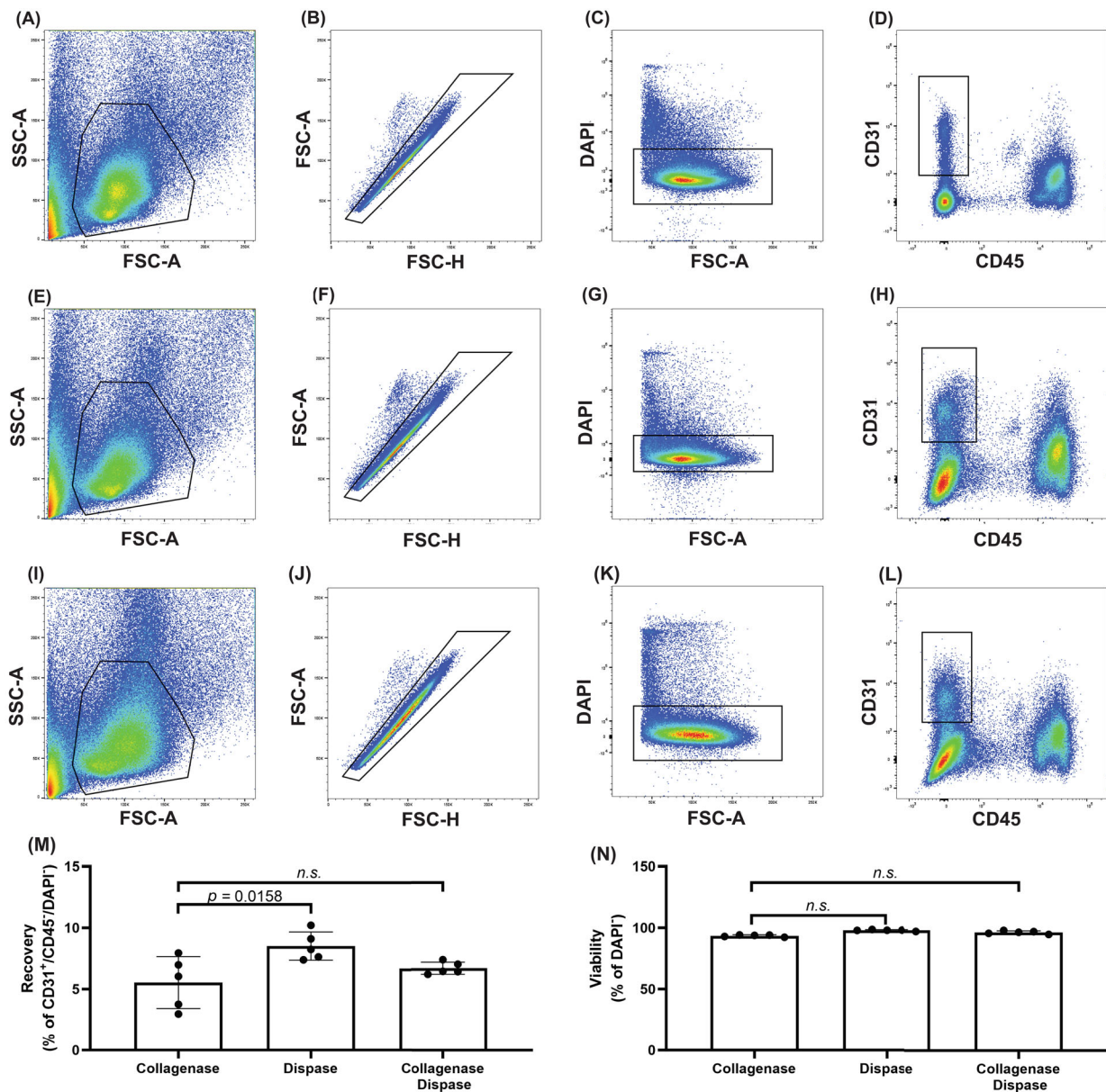


FIGURE 7 Recovery of live lung endothelial cells comparing collagenase-based and dispase-based tissue dissociation protocols using DAPI exclusion. Live endothelial cells were identified by flow cytometry in single-cell suspensions prepared from lung tissue of adult (22 week-old) mice that was dissociated using either collagenase (A–D) or dispase (E–H), or combinations thereof (I–L). Primary debris exclusion was undertaken by SSC-A versus FCS-A gating (A, E, I), followed by doublet exclusion using FSC-A versus FSC-H gating (B, F, J). Live cells were identified by DAPI exclusion, thus, represented by DAPI⁻ events (C, G, K), and CD31⁺/CD45⁻ events represented endothelial cells (D, H, L). Live endothelial cell recovery was assessed as (M) a percentage of CD31⁺/CD45⁻/DAPI⁻ events: the gated populations in C versus D, G versus H, or K versus L. The viability of the whole single-cell suspension was assessed as (N) a percentage of DAPI⁻ events in the singlet cell population event gate: the gated populations in C versus B, G versus F, and K versus J. For each cell population, 300,000 events were assessed ($n = 5$ experimental animals per group). Statistical comparisons were made using a one-way ANOVA with Tukey's post hoc test. $p < 0.05$ was considered significant. n.s., not significant. [Color figure can be viewed at wileyonlinelibrary.com]

approach. Our comparison of the DAPI exclusion and Hoechst inclusion approaches for the assessment of cell viability provided an interesting insight into whether one of these approaches may be better than the other, for the determination of cell viability. Using Hoechst inclusion to identify live cells, a small (12%) but significant ($p = 0.0029$) reduction in the viability of the complete single-cell suspension (which includes inflammatory and epithelial cells) was noted

in the dispase group. This was not detected using DAPI exclusion to assess cell viability. These data would suggest that Hoechst is a better method for the assessment of cell viability than is DAPI, using flow cytometry. A possible explanation for the apparently higher sensitivity of Hoechst 33342 is that live cells are Hoechst 33342-permeable [38], but not DAPI-permeable [39]. While Hoechst 33342 will diffuse into live cells; cells in the process of dying

are variably permeable to DAPI, which is further impacted by the manner of cell death (apoptosis versus necrosis). As such, Hoechst 33342 appears to be the agent of choice to assess cell viability. However, DAPI was more routinely employed in this study, as Hoechst 33342 requires longer incubation times (which is undesirable when working with live cells intended for subsequent gene expression analysis) than does DAPI, and Hoechst 33342 staining requires an incubation temperature of 37°C, while DAPI can be incubated with cells at room temperature.

Interestingly, examining the onset of apoptosis by screening for translocation of phosphatidylserine, an early apoptosis marker detected with annexin V, revealed that early apoptosis was detected in twice as many endothelial cells recovered with collagenase than in endothelial cells recovered with dispase. Initially, this may seem counter-intuitive, given the markedly improved recovery of live endothelial cells using collagenase, described above. However, the authors speculate that amongst the many lost endothelial cells in the dispase-dissociated tissue were endothelial cells undergoing apoptosis. This had not been experimentally proven in this report.

In the spirit of refining, reducing, and replacing experimental animals in studies on human disease, it is desirable to extract as much experimental material as possible from an experimental run. To this end, the recovery of another lung cell-type, the epithelial cell, from the single-cell suspensions generated by collagenase or dispase-mediated tissue dissociation was also evaluated. In contrast to endothelial cells, dispase-mediated tissue dissociation yielded ≈ 9 -fold more live epithelial cells than did the collagenase approach. Two explanations might be proposed to clarify this. The collagenase may have been unable to release sufficient numbers of epithelial cells from the lung tissue, or, given the presence of an intermediate “cloud” in Figure 4E, the collagenase may not have been able to adequately unmask the EpCam epitope on the lung epithelial cells. Interestingly, in contrast to the observations with endothelial cells, a mixture of collagenase and dispase highlighted dispase as the enzyme preparation of choice for the recovery of epithelial cells from the lungs of developing mouse pups. Similar to the explanations proposed for endothelial cell recovery, discussed above; dispase might be a more appropriate enzyme preparation for the degradation of matrix molecules that embed epithelial cells in the epithelial lining of the conducting airways and in the distal airspaces of the lung; or, that the collagenase is inefficient at liberating epithelial cells from tissue, and at the same time, proteolytically degrades collagenase. In view of the observations made for endothelial cell recovery with a collagenase-dispase mixture (above), it appears unlikely that this last possibility: that collagenase and dispase degrade one another, is the likely explanation. It appears more likely that in young, developing mouse pups, collagenase is simply better at liberating endothelial cells from the vascular matrix, while dispase is better at liberating epithelial cells from the apical surfaces of the proximal airways and distal airspaces. In sum, these data indicate that while the collagenase tissue dissociation approach is superior to the dispase approach for the isolation of lung endothelial cells, the reverse is true for lung epithelial cells.

Endothelial cells in general [16], and, in the context of the present study, lung endothelial cells in particular [21], do not represent a

homogenous population of a single endothelial cell-type. Rather, endothelial cell pools from any organ will include those derived from the arterial and venous circulation, the capillary beds, the lymphatic circulation, as well as endothelial progenitor cells. Each of these endothelial cell subtypes express a discrete set of markers that can be used to identify each subtype [21]. In the present study, those endothelial cell subtype markers were used to determine whether the collagenase- or dispase-based tissue dissociation protocols impacted the subtype composition of recovered endothelial cells pools. Using PCA of single-cell RNA-Seq data, nine different endothelial subtype clusters were noted in endothelial cell pools recovered from lung tissue dissociated with collagenase and dispase. Among the endothelial cell clusters identified were three groups of arterial-derived endothelial cells: one marked by *Acta2* and *Tagln*, a second group marked by *Wnt5a*, *Tgfb1*, and *P2ry14*, and a third group marked by *Mtap4* and *Gpc3*. Three groups of capillary endothelial cells were also identified, the alveolar (a) capillary (aCap; also called aerocytes) marked by *Car4* and *Ednrb*, and two groups of general (g) capillary (gCap) endothelial cells, the first group marked by *Sema3* and *Sox17*, and the second group marked by histocompatibility antigens. Venous endothelial cells were also identified, marked by multiple fibulins; as were lymphatic endothelial cells marked by *Mmm1* and *Fxyd6*. A ninth cluster was also identified, which expressed a number of genes that are associated with progenitor cells, and hence, are termed “progenitors” here.

While all nine clusters of endothelial cell subtypes were identified in endothelial cell pools recovered using both the collagenase and dispase approaches, differences in the cell subtype composition of recovered endothelial cell pools was noted comparing the two approaches. Endothelial cell pools generated with collagenase exhibited marked heterogeneity with a robust (>10% of total cells) presence of arterial, venous, and capillary endothelial cells. In contrast, endothelial cell pools generated with dispase exhibited a pronounced (>75% of total cells) representation of one subset of general capillary endothelial cells, but comparatively poor representation of other endothelial cell subtypes. Why collagenase and dispase may differentially impact endothelial cell recovery, viability, and subtype composition of recovered endothelial cell pools might be attributed to two separate phenomena, or a combination thereof. First, the two enzyme preparations might have different efficacy at liberating endothelial cells from vascular tissue, ostensibly through the degradation of extracellular matrix and cell contacts. Alternatively, the two enzyme preparations might have different capacities for degrading cell-surface epitopes, which would impact the ability of fluorescently-conjugated antibodies to bind to –and thus, facilitate the detection of– different cell types. These two phenomena have recently been discussed at length in the pages of this journal [29], in the context of enzymatic dissociation of peripheral human lung tissue for the generate of single-cell suspensions of lung cells.

A key limitation of this study is that an impact of collagenase on endothelial cell gene expression (vs. endothelial cells from lungs not enzymatically digested) was not assessed, since endothelial cell recovery without enzymatic digestion is not possible. It may well be that the gene expression patterns reflected in the single cell analyses are not the same patterns present in endothelial cell in lungs not exposed

to collagenase. This must be kept in mind in gene profiling studies that employ enzymatic digestion of tissue for cell recovery.

The data presented in the current study give rise to the question: should tissue dissociation protocols for endothelial cell isolation be standardized? While standardization has its merits, there is also still much to be learned about the impact of different tissue dissociation protocols on endothelial cell recovery, diversity of the recovered endothelial cell pools, and gene expression in recovered cells. Thus, at this point in time, the investigators feel that a diversity of approaches will be instructive, with the caveat that those approaches must be described in detail in published reports, to facilitate an appreciation of the comparability of the datasets generated with different tissue dissociation protocols.

In sum, collectively, the data presented here indicate that the collagenase and dispase approaches to tissue dissociation for endothelial cell isolation from developing mouse lungs yield a markedly different endothelial subtype composition of recovered endothelial cell pools. Collectively, the data presented in this report suggest that *C. histolyticum* collagenase A yields a superior endothelial cell pool recovery from the developing lungs of mouse pups, in terms of cell number, cell viability, and endothelial cell subtype complexity than does dispase. However, dispase-based approaches appear more suitable for endothelial cell recovery from adult mouse lungs.

AUTHOR CONTRIBUTIONS

Rory E. Morty: Resources; supervision; project administration; formal analysis; writing – review and editing; writing – original draft; funding acquisition; conceptualization. **Francesco Palumbo:** Conceptualization; investigation; writing – original draft; writing – review and editing; visualization; validation; methodology; formal analysis; data curation; supervision. **Miša Gunjak:** Conceptualization; methodology; data curation; investigation; validation; formal analysis. **Patty J. Lee:** Resources; supervision; data curation; formal analysis; visualization; writing – review and editing; writing – original draft; funding acquisition; conceptualization; investigation. **Stefan Günther:** Conceptualization; writing – review and editing; validation; methodology; visualization; software; formal analysis; data curation; resources; investigation. **Anne Hilgendorff:** Resources; supervision; data curation; formal analysis; project administration; writing – review and editing; funding acquisition; visualization; conceptualization; investigation. **István Vadász:** Conceptualization; funding acquisition; writing – original draft; writing – review and editing; data curation; resources; project administration; formal analysis. **Susanne Herold:** Conceptualization; writing – original draft; funding acquisition; writing – review and editing; visualization; methodology; validation; formal analysis; project administration; data curation; resources. **Werner Seeger:** Conceptualization; data curation; formal analysis; supervision; funding acquisition; project administration; writing – original draft. **Christian Mühlfeld:** Conceptualization; writing – original draft; funding acquisition; writing – review and editing; validation; methodology; project administration; formal analysis; data curation; resources; investigation.

ACKNOWLEDGMENTS

This work was supported by the German Federal Ministry of Education and Research (DZL-TLRC; DZL-BREATH, DZL-UGMLC, DZL-CPC); the German Research Foundation: (197785619, 114933180, 284237345, 390649896, and 420759458); Heidelberg University Hospital; the Hessian Ministry of Higher Education, Research and the Arts (LOEWE: III L7-519/05.00.002); the Max Planck Society (MPI-HLR); the Medical Faculty of the University of Heidelberg; the U. S. National Heart, Lung and Blood Institute of the National Institutes of Health (R01HL138386); the U.S. Department of Veterans Affairs (VAORD11858595); the U.S. Department of Defense (PR150809); and the von Berhing-Röntgen Foundation: 66-LV07.

The authors acknowledge the outstanding support from Dr. Monika Langlotz and the Flow Cytometry & FACS core facility of the Zentrum für Molekulare Biologie der Universität Heidelberg, Heidelberg, Germany; from the Deep Sequencing Platform and the Flow Cytometry and Cell Sorting Facility of the Max Planck Institute for Heart and Lung Research, Bad Nauheim, Germany; from Dr. Verena Rickert-Zacharias, Scientific Coordinator of the Department of Translational Pulmonology, Heidelberg University Hospital, Heidelberg, Germany; and from the Flow Cytometry Core Facility, School of Life Sciences, École Polytechnique Fédérale de Lausanne (EPFL), Lausanne, Switzerland. Open Access funding enabled and organized by Projekt DEAL.

CONFLICT OF INTEREST STATEMENT

The authors declare no potential conflicts of interest.

PEER REVIEW

The peer review history for this article is available at <https://www.webofscience.com/api/gateway/wos/peer-review/10.1002/cyto.a.24843>.

ORCID

Francesco Palumbo  <https://orcid.org/0000-0002-5352-6773>

Miša Gunjak  <https://orcid.org/0000-0001-5179-1605>

Patty J. Lee  <https://orcid.org/0000-0001-9906-1628>

Stefan Günther  <https://orcid.org/0000-0002-5594-4549>

Anne Hilgendorff  <https://orcid.org/0000-0002-3725-996X>

István Vadász  <https://orcid.org/0000-0003-1370-9783>

Susanne Herold  <https://orcid.org/0000-0001-6343-0911>

Werner Seeger  <https://orcid.org/0000-0003-1946-0894>

Christian Mühlfeld  <https://orcid.org/0000-0002-7827-4867>

Rory E. Morty  <https://orcid.org/0000-0003-0833-9749>

REFERENCES

1. Kina YP, Khadim A, Seeger W, El Agha E. The lung vasculature: a driver or passenger in lung branching morphogenesis? *Front Cell Dev Biol.* 2020;8:623868.
2. Appuhn SV, Siebert S, Myti D, Wrede C, Surate Solaligue DE, Perez-Bravo D, et al. Capillary changes precede disordered alveolarization in a mouse model of bronchopulmonary dysplasia. *Am J Respir Cell Mol Biol.* 2021;65:81–91.
3. Labode J, Dullin C, Wagner WL, Myti D, Morty RE, Mühlfeld C. Evaluation of classifications of the monopodial bronchopulmonary vasculature using clustering methods. *Histochem Cell Biol.* 2022;158:435–45.

4. Rao S, Liu M, Iosef C, Knutsen C, Alvira CM. Endothelial-specific loss of IKKbeta disrupts pulmonary endothelial angiogenesis and impairs postnatal lung growth. *Am J Physiol Lung Cell Mol Physiol.* 2023;325:L299–313.
5. Thebaud B, Abman SH. Bronchopulmonary dysplasia: where have all the vessels gone? Roles of angiogenic growth factors in chronic lung disease. *Am J Respir Crit Care Med.* 2007;175:978–85.
6. Zanini F, Che X, Knutsen C, Liu M, Suresh NE, Domingo-Gonzalez R, et al. Developmental diversity and unique sensitivity to injury of lung endothelial subtypes during postnatal growth. *iScience.* 2023;26:106097.
7. Hilgendorff A, Apitz C, Bonnet D, Hansmann G. Pulmonary hypertension associated with acute or chronic lung diseases in the preterm and term neonate and infant. The European paediatric pulmonary vascular disease network, endorsed by ISHLT and DGPK. *Heart.* 2016;102(Suppl 2):ii49–56.
8. Goldenberg NM, Kuebler WM. Endothelial cell regulation of pulmonary vascular tone, inflammation, and coagulation. *Compr Physiol.* 2015;5:531–59.
9. Birukov KG, Karki P. Injured lung endothelium: mechanisms of self-repair and agonist-assisted recovery (2017 Grover conference series). *Pulm Circ.* 2018;8:2045893217752660.
10. Bazan IS, Kim SJ, Ardito TA, Zhang Y, Shan P, Sauler M, et al. Sex differences and altered mitophagy in experimental pulmonary hypertension. *Am J Physiol Lung Cell Mol Physiol.* 2022;322:L761–9.
11. Cantu A, Cantu Gutierrez M, Zhang Y, Dong X, Lingappan K. Endothelial to mesenchymal transition in neonatal hyperoxic lung injury: role of sex as a biological variable. *Physiol Genomics.* 2023;55:345–54.
12. Tsikis ST, Hirsch TI, Fligor SC, Quigley M, Puder M. Targeting the lung endothelial niche to promote angiogenesis and regeneration: a review of applications. *Front Mol Biosci.* 2022;9:1093369.
13. Bandyopadhyay G, Huyck HL, Misra RS, Bhattacharya S, Wang Q, Mereness J, et al. Dissociation, cellular isolation, and initial molecular characterization of neonatal and pediatric human lung tissues. *Am J Physiol Lung Cell Mol Physiol.* 2018;315:L576–83.
14. Grant D, Wanner N, Frimel M, Erzurum S, Asosingh K. Comprehensive phenotyping of endothelial cells using flow cytometry 1: murine. *Cytometry A.* 2021;99:251–6.
15. Grant D, Wanner N, Frimel M, Erzurum S, Asosingh K. Comprehensive phenotyping of endothelial cells using flow cytometry 2: human. *Cytometry A.* 2021;99:257–64.
16. Kalucka J, de Rooij L, Goveia J, Rohlenova K, Dumas SJ, Meta E, et al. Single-cell transcriptome atlas of murine endothelial cells. *Cell.* 2020;180(4):e20.
17. Raredon MSB, Adams TS, Suhail Y, Schupp JC, Poli S, Neumark N, et al. Single-cell connectomic analysis of adult mammalian lungs. *Sci Adv.* 2019;5:eaaw3851.
18. Schupp JC, Adams TS, Cosme C Jr, Raredon MSB, Yuan Y, Omote N, et al. Integrated single-cell atlas of endothelial cells of the human lung. *Circulation.* 2021;144:286–302.
19. He L, Vanlandewijck M, Mae MA, Andrae J, Ando K, Del Gaudio F, et al. Single-cell RNA sequencing of mouse brain and lung vascular and vessel-associated cell types. *Sci Data.* 2018;5:180160.
20. Negretti NM, Plosa EJ, Benjamin JT, Schuler BA, Habermann AC, Jetter CS, et al. A single-cell atlas of mouse lung development. *Development.* 2021;148(24):dev199512.
21. Gillich A, Zhang F, Farmer CG, Travaglini KJ, Tan SY, Gu M, et al. Capillary cell-type specialization in the alveolus. *Nature.* 2020;586:785–9.
22. Reichard A, Asosingh K. Best practices for preparing a single cell suspension from solid tissues for flow cytometry. *Cytometry A.* 2019;95:219–26.
23. Marsh LM, Cakarova L, Kwapiszewska G, Von Wulffen W, Herold S, Seeger W, et al. Surface expression of CD74 by type II alveolar epithelial cells: a potential mechanism for macrophage migration inhibitory factor-induced epithelial repair. *Am J Physiol Lung Cell Mol Physiol.* 2009;296:L442–52.
24. Niethamer TK, Stabler CT, Leach JP, Zepp JA, Morley MP, Babu A, et al. Defining the role of pulmonary endothelial cell heterogeneity in the response to acute lung injury. *Elife.* 2020;9:1–28.
25. Singer BD, Mock JR, D'Alessio FR, Aggarwal NR, Mandke P, Johnston L, et al. Flow-cytometric method for simultaneous analysis of mouse lung epithelial, endothelial, and hematopoietic lineage cells. *Am J Physiol Lung Cell Mol Physiol.* 2016;310:L796–801.
26. Donati Y, Blaskovic S, Ruchonnet-Metrailler I, Lascano Maillard J, Barazzone-Argiroffo C. Simultaneous isolation of endothelial and alveolar epithelial type I and type II cells during mouse lung development in the absence of a transgenic reporter. *Am J Physiol Lung Cell Mol Physiol.* 2020;318:L619–30.
27. Hurskainen M, Mizikova I, Cook DP, Andersson N, Cyr-Depauw C, Lesage F, et al. Single cell transcriptomic analysis of murine lung development on hyperoxia-induced damage. *Nat Commun.* 2021;12:1565.
28. Tighe RM, Redente EF, Yu YR, Herold S, Sperling AI, Curtis JL, et al. Improving the quality and reproducibility of flow cytometry in the lung. An official American thoracic society workshop report. *Am J Respir Cell Mol Biol.* 2019;61:150–61.
29. Bondonese A, Craig A, Fan L, Valenzi E, Bain W, Lafyatis R, et al. Impact of enzymatic digestion on single cell suspension yield from peripheral human lung tissue. *Cytometry A.* 2023;103:777–85.
30. Bruning RS, Tombor L, Schulz MH, Dimmeler S, John D. Comparative analysis of common alignment tools for single-cell RNA sequencing. *Gigascience.* 2022;1–12.
31. Dobin A, Davis CA, Schlesinger F, Drenkow J, Zaleski C, Jha S, et al. STAR: ultrafast universal RNA-seq aligner. *Bioinformatics.* 2013;29:15–21.
32. Wolf FA, Angerer P, Theis FJ. SCANPY: large-scale single-cell gene expression data analysis. *Genome Biol.* 2018;19:15.
33. Fehrenbach ML, Cao G, Williams JT, Finklestein JM, Delisser HM. Isolation of murine lung endothelial cells. *Am J Physiol Lung Cell Mol Physiol.* 2009;296:L1096–103.
34. Dylag AM, Misra RS, Bandyopadhyay G, Poole C, Huyck HL, Jehri MG, et al. New insights into the natural history of bronchopulmonary dysplasia from proteomics and multiplexed immunohistochemistry. *Am J Physiol Lung Cell Mol Physiol.* 2023;325:L419–33.
35. Schittny JC. Development of the lung. *Cell Tissue Res.* 2017;367:427–44.
36. Shapiro SD, Endicott SK, Province MA, Pierce JA, Campbell EJ. Marked longevity of human lung parenchymal elastic fibers deduced from prevalence of D-aspartate and nuclear weapons-related radiocarbon. *J Clin Invest.* 1991;87:1828–34.
37. Ahsan T, Harwood F, McGowan KB, Amiel D, Sah RL. Kinetics of collagen crosslinking in adult bovine articular cartilage. *Osteoarthritis Cartilage.* 2005;13:709–15.
38. Darzynkiewicz Z, Bruno S, Del Bino G, Gorczyca W, Hotz MA, Lassota P, et al. Features of apoptotic cells measured by flow cytometry. *Cytometry.* 1992;13:795–808.
39. Kepp O, Galluzzi L, Lipinski M, Yuan J, Kroemer G. Cell death assays for drug discovery. *Nat Rev Drug Discov.* 2011;10:221–37.

SUPPORTING INFORMATION

Additional supporting information can be found online in the Supporting Information section at the end of this article.

How to cite this article: Palumbo F, Gunjak M, Lee PJ, Günther S, Hilgendorff A, Vadász I, et al. Impact of different tissue dissociation protocols on endothelial cell recovery from developing mouse lungs. *Cytometry.* 2024. <https://doi.org/10.1002/cyto.a.24843>